A novel methodology for constructing a multi-wing chaotic and hyperchaotic system with a unified step function switching control*

Chao-Xia Zhang(张朝霞)[1] and Si-Min Yu(禹思敏)[2,†]

[1] *Department of Computer Science, Guangdong University of Education, Guangzhou* 510303, *China*
[2] *Faculty of Automation, Guangdong University of Technology, Guangzhou* 510006, *China*

(Received 17 November 2015; revised manuscript received 26 January 2016; published online 5 April 2016)

This paper aims at developing a novel method of constructing a class of multi-wing chaotic and hyperchaotic system by introducing a unified step function. In order to overcome the essential difficulties in iteratively adjusting multiple parameters of conventional multi-parameter control, this paper introduces a unified step function controlled by a single parameter for constructing various multi-wing chaotic and hyperchaotic systems. In particular, to the best of the authors' knowledge, this is also the first time to find a non-equilibrium multi-wing hyperchaotic system by means of the unified step function control. According to the heteroclinic loop Shilnikov theorem, some properties for multi-wing attractors and its chaos mechanism are further discussed and analyzed. A circuit for multi-wing systems is designed and implemented for demonstration, which verifies the effectiveness of the proposed approach.

Keywords: non-equilibrium multi-wing hyperchaotic system, single parameter control, unified step function, circuit implementation

PACS: 05.45.Gg, 05.45.Pq **DOI:** 10.1088/1674-1056/25/5/050503

1. Introduction

Chaos control refers to purposefully eliminating or weakening chaotic behavior of a system through some control methods when the chaotic motion is harmful. Since the Ott–Grebogi–Yorke (OGY) method was proposed in 1990,[1] much effort has been devoted to the study of controlling chaos. However, not all chaotic behaviors are harmful, and recent research has shown that chaos can actually be useful under certain circumstances, such as chaos-based multimedia encryption and decryption.[2,3] Therefore, chaotification by making an originally non-chaotic dynamical system chaotic, enhancing existing chaos, or extending the number of saddle focus equilibria for generating multi-wing or multi-scroll chaotic and hyperchaotic systems has attracted some special attention in recent years.[4–13]

Compared with the double wing chaotic system, the multi-wing chaotic system is a new type of generalized Lorenz system characterized by multiple wings which are distributed in a single direction or in multiple directions, the phase portrait for multi-wing chaotic attractor is formed with nested wing, the number and the grid distribution of the wing can be adjusted by parameters.[10] In contrast to the double-wing chaotic system, the multi-wing chaotic system possesses the following features that have potential applications in secure communication: i) the phase trajectories of multi-wing chaotic attractors can randomly jump in all wings with ergodic property, so that the dynamical behavior is more complicated than those of Lorenz system and Chen system, and the statistical properties can be improved; ii) by introducing a nonlinear-function controller, several key parameters of multi-wing chaotic attractors can be easily adjusted, including the width of each segment, amplitude, slope, equilibrium, and turning points. As a result, one can easily control the system equilibrium, the number of scrolls, the shapes and sizes of the scrolls, the spatial distribution of the scrolls, and even the phase trajectories.

It is noticed that, up to now, multiple parameter nonlinear function switching controllers, such as duality-symmetric multi-segment linear function and multi-segment quadratic function, have usually been considered for generating multi-wing chaotic attractors from autonomous three-dimensional (3D) quadratic double-wing chaotic systems as shown in Fig. 1.[10–12] However, there exist the following aspects for improving this kind of switching control method.

(i) Different kinds of multi-segment linear functions and multi-segment quadratic functions are needed for generating different multi-wing chaotic systems, and a unified controller is not formed and the construction criterion is complicated.

(ii) Nonlinear function $F(\xi)$ has multiple parameters F_i $(i = 0, 1, 2, \ldots)$ to be determined when E_i $(i = 1, 2, 3, \ldots)$ in horizontal direction are given.

(iii) Parameters F_i influence each other, when one parameter varies, other coupled parameters also change correspondingly.

*Project supported by the National Natural Science Foundation of China (Grant No. 61403143), the Natural Science Foundation of Guangdong Province, China (Grant No. 2014A030313739), the Science and Technology Foundation Program of Guangzhou City, China (Grant No. 201510010124), and the Excellent Doctorial Dissertation Foundation of Guangdong Province, China (Grant No. XM080054).

†Corresponding author. E-mail: siminyu@163.com

© 2016 Chinese Physical Society and IOP Publishing Ltd

(iv) Algorithm is complex, all parameters F_i $(i = 0,1,2,\ldots)$ are determined by trial-and-error approach, and the repeated iterations are needed to obtain an appropriate set of parameter values.

To cope with the above-mentioned issues, this paper introduces a new step function control method with a single parameter ε, which is characterized by the following two aspects.

(i) There is a unified step function $g(y,\varepsilon)$ for constructing various multi-wing chaotic and hyperchaotic systems, and the construction method is simple and practical.

(ii) Single parameter ε controller is adopted. When $y_i = W_i$ $(i = 1,2,3,\ldots)$ in horizontal direction are given, once ε is determined, various n $(n = 3,4)$-dimensional multi-wing chaotic and hyperchaotic systems can be constructed.

Based on this single parameter ε step function control method, this paper constructs an absolute value piecewise linear 3D multi-wing chaotic system, a square 3D multi-wing chaotic system and a square four-dimensional (4D) multi-wing hyperchaotic system, respectively. According to the heteroclinic loop Shilnikov theorem,[14] the chaos mechanism of absolute value piecewise linear 3D multi-wing chaotic system is analyzed, a circuit for both absolute value piecewise linear and square 3D multi-wing chaotic systems is designed and implemented.

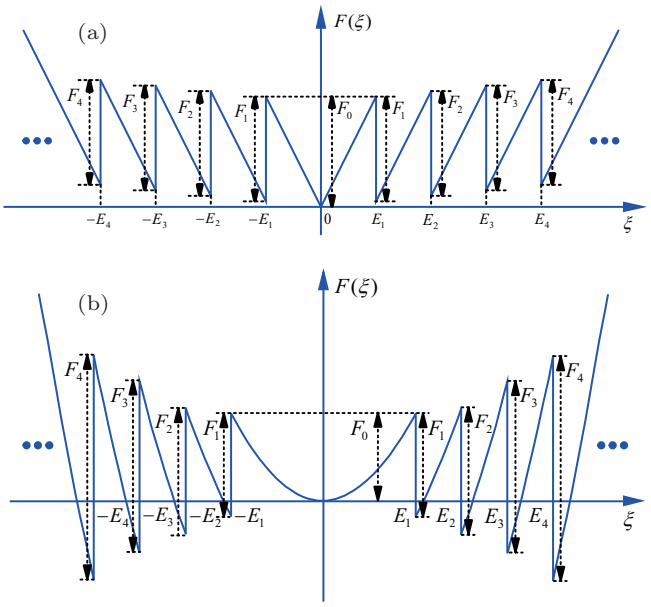


Fig. 1. (color online) Multiple parameter nonlinear functions: (a) multi-segment linear function and (b) multi-segment square function.

Most reported chaotic systems, i.e., Lorenz system, Chen system, etc, have a limited number of equilibria.[15–18] Therefore, chaos in these systems can be proved by using conventional Shilnikov theorem, in which at least one unstable equilibrium point for emergence of chaos is required. However, it is impossible to use the conventional Shilnikov theorem to verify the chaos in non-equilibrium systems. According to Shilnikov theorem, one or more saddle focus equilibria are keys to the formations of heteroclinic orbit and heteroclinic loop in a chaotic system.[14] For example, double-wing chaotic attractors are formed from saddle or saddle focus equilibria in generalized Lorenz system family,[15–18] and multi-wing chaotic attractors can be constructed by extending the number of saddle focus equilibria.[10–12] As is well known, heteroclinic orbit and heteroclinic loop cannot be formed if there is no equilibrium point. It is noticed that a 4D multi-wing chaotic system was recently found to have no equilibrium point.[19] However, to the best of the authors' knowledge, there has been no report about a 4D multi-wing hyperchaotic system without equilibrium point so far. One may ask whether there is a possible way further to find a non-equilibrium 4D multi-wing hyperchaotic system. This paper gives a positive answer to the question.

In spite of the fact that a simple non-equilibrium chaotic system was found in 1994,[20] studies on chaotic systems without equilibrium have only bloomed recently.[21,22] It is worth noting that such a chaotic system without equilibrium is categorized as a chaotic system with hidden attraction because its basin of attraction does not intersect with small neighborhoods of any equilibrium.[23] Owing to their academic significance and practical importance, studying systems with hidden attractors has received significant attention.[24]

The rest of the paper is organized as follows. Construction of multi-wing chaotic and hyperchaotic systems via a unified single parameter ε step function control is introduced in Section 2. Some properties of a multi-wing system are discussed and analyzed in Section 3. Circuit design and implementation are demonstrated in Section 4. Finally, in Section 5 some conclusions are drawn.

2. Construction of multi-wing chaotic and hyperchaotic systems via a unified single parameter ε step function control

In this section, two types of double-wing chaotic systems and one type of double-wing hyperchaotic system are first considered. Then, the corresponding multi-wing chaotic system and hyperchaotic system based on a unified single parameter ε step function control are introduced, and the construction criterion for the unified step function is also given.

2.1. Double-wing chaotic and hyperchaotic systems

According to the generalized Lorenz system family,[13–16] two types of double-wing chaotic systems and one type of double-wing hyperchaotic system are given at first. From these systems, one can further obtain the corresponding multi-wing chaotic and hyperchaotic systems by a unified step function switching control.

The n $(n = 3,4)$-dimensional double wing chaotic or hy-

perchaotic system is in the form of

$$\begin{cases} \dot{x}_1 = f_1(x_1, x_2, \ldots, x_n), \\ \vdots \\ \dot{x}_{n-1} = f_{n-1}(x_1, x_2, \ldots, x_n), \\ \dot{x}_n = \xi_{n1} h(x_2) - \xi_{n2} x_n, \end{cases} \tag{1}$$

where $h(x_2) \in \{|x_2|, x_2^2\}$ is an even-symmetric function, ξ_{n1} and ξ_{n2} are constants, $f_1(x_1, x_2, \ldots, x_{n-1})$ is a linear function, and $f_i(x_1, x_2, \ldots, x_n)$ $(i = 2, 3, \ldots, n)$ are piecewise linear function or quadratic polynomial. Furthermore, $f_1(x_1, x_2, \ldots, x_n), \ldots, f_{n-1}(x_1, x_2, \ldots, x_n)$ can make Eq. (1) invariant under the transformation of $(x, y, z) \to (-x, -y, z)$.

According to Eq. (1), let $n = 3$, $f_1(x_1, x_2, x_3)$ is a linear function, $f_2(x_1, x_2, x_3)$ is a piecewise linear function, $h(x_2)$ is an absolute value function, one can obtain the absolute value piecewise linear 3D double wing chaotic system as

$$\begin{cases} \dot{x} = -a_{11} x + a_{12} y, \\ \dot{y} = \mathrm{sgn}(x)(a_{21} - z) + a_{22} y, \\ \dot{z} = a_{31} |y| - a_{32} z, \end{cases} \tag{2}$$

where $a_{11} = 1.18$, $a_{12} = 1.18$, $a_{21} = 5.82$, $a_{22} = 0.7$, $a_{31} = 4$, and $a_{32} = 0.168$.

It is noticed that the third equation in Eq. (2) includes an even-symmetric absolute value term $a_{31}|y|$ and a linear term $a_{32}z$, which can generate a multi-wing chaotic system by a unified step function switching control.

According to Eq. (1), let $n = 3$, $f_1(x_1, x_2, x_3)$ is a linear function, $f_2(x_1, x_2, x_3)$ is a quadratic polynomial, $h(x_2)$ is a square function, one can obtain the square 3D double wing chaotic system as

$$\begin{cases} \dot{x} = -d_{11} x + d_{12} y, \\ \dot{y} = -d_{21} xz + d_{22} y, \\ \dot{z} = d_{31} y^2 - d_{32} z, \end{cases} \tag{3}$$

where $d_{11} = 36$, $d_{12} = 36$, $d_{21} = 20$, $d_{22} = 20$, $d_{31} = 100$, and $d_{32} = 3$.

It is noticed that the third equation in Eq. (3) includes an even-symmetric square term $d_{31}y^2$ and a linear term $d_{32}z$, which can generate multi-wing chaotic system by a unified step function switching control.

According to Eq. (1), let $n = 4$, $f_1(x_1, x_2, x_3, x_4)$ is a linear function, $f_2(x_1, x_2, x_3, x_4)$ and $f_3(x_1, x_2, x_3, x_4)$ are both quadratic polynomials, $h(x_2)$ is a square function, one can obtain the general form of a square 4D double wing hyperchaotic system as

$$\begin{cases} \dot{x} = -b_{11} x + b_{12} y + b_{13} z, \\ \dot{y} = -b_{21} xu + b_{22} y, \\ \dot{z} = b_{31} xu + b_{32} z, \\ \dot{u} = b_{41} y^2 - b_{42} u, \end{cases} \tag{4}$$

where $b_{11} = 36$, $b_{12} = 45$, $b_{13} = 3.5$, $b_{21} = 5.6$, $b_{22} = 20$, $b_{31} = 0.5$, $b_{32} = 0.3$, $b_{41} = 17.9$, and $b_{42} = 3$.

It is noticed that the fourth equation in Eq. (4) includes an even-symmetric square term $b_{41}y^2$ and a linear term $b_{42}u$, which can generate a multi-wing hyperchaotic system by a unified step function switching control.

Based on Eqs. (2)–(4), the numerical simulation results of double-wing chaotic and hyperchaotic attractors are shown in Fig. 2. The Lyapunov exponents of the absolute value piecewise linear 3D double wing chaotic system are $\mathrm{LE}_1 = 0.41$, $\mathrm{LE}_2 = 0.00$, and $\mathrm{LE}_3 = -1.05$; the Lyapunov exponents of the square 3D double wing chaotic system are $\mathrm{LE}_1 = 1.36$, $\mathrm{LE}_2 = 0.00$, $\mathrm{LE}_3 = -20.36$; the Lyapunov exponents of the square 4D double wing hyperchaotic system are $\mathrm{LE}_1 = 0.99$, $\mathrm{LE}_2 = 0.35$, $\mathrm{LE}_3 = 0.00$, and $\mathrm{LE}_4 = -20.05$.

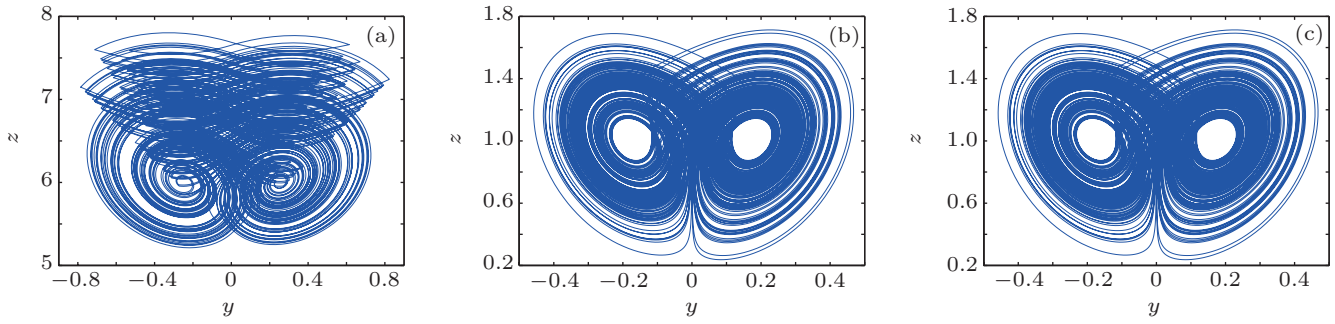


Fig. 2. (color online) Double-wing attractors of chaotic and hyperchaotic system: (a) double-wing attractor of absolute value piecewise linear 3D chaotic system; (b) double-wing attractor of square 3D chaotic system; (c) double-wing attractor of square 4D hyperchaotic system.

2.2. Generation of multi-wing chaotic and hyperchaotic systems via a unified single parameter ε step function control

According to Eqs. (2)–(4), by adding a unified single parameter ε step function controller $g_i(y, \varepsilon)$ $(i = 1, 2, 3)$ to the last equation, one can obtain the corresponding three types of multi-wing chaotic and hyperchaotic systems.

Based on Eq. (2), an absolute value piecewise linear 3D multi-wing chaotic system controlled by $g_1(y, \varepsilon)$ is given by

$$\begin{cases} \dot{x} = -a_{11} x + a_{12} y, \\ \dot{y} = \mathrm{sgn}(x)(a_{21} - z) + a_{22} y, \\ \dot{z} = a_{31} |y| - a_{32} z - g_1(y, \varepsilon), \end{cases} \tag{5}$$

where parameters a_{ij} are the same as those in Eq. (2).

Based on Eq. (3), a square 3D multi-wing chaotic system controlled by $g_2(y,\varepsilon)$ is given by

$$\begin{cases} \dot{x} = -d_{11}x + d_{12}y, \\ \dot{y} = -d_{21}xz + d_{22}y, \\ \dot{z} = d_{31}y^2 - d_{32}z - g_2(y,\varepsilon), \end{cases} \tag{6}$$

where parameters d_{ij} are the same as those in Eq. (3).

Based on Eq. (4), a square 4D multi-wing hyperchaotic system controlled by $g_3(y,\varepsilon)$ is given by

$$\begin{cases} \dot{x} = -b_{11}x + b_{12}y + b_{13}z, \\ \dot{y} = -b_{21}xu + b_{22}y, \\ \dot{z} = b_{31}xu + b_{32}z, \\ \dot{u} = b_{41}y^2 - b_{42}u - g_3(y,\varepsilon), \end{cases} \tag{7}$$

where parameter b_{ij} are the same as those in Eq. (4).

Among Eqs. (5)–(7), let the general form of a unified single parameter ε even-symmetric step function controller be

$$g_i(y,\varepsilon) = \sum_{k=1}^{M} H_k(\varepsilon)\mathrm{step}(y - W_k) + \sum_{k=1}^{M} H_k(\varepsilon)\mathrm{step}(-y - W_k), \tag{8}$$

where $i = 1,2,3$, $H_k(\varepsilon)$ $(k = 1,2,\ldots,M)$ are altitudes of the step function, ε is a single parameter, W_k $(k = 1,2,\ldots,M)$ are jump point coordinates of the step function, $\mathrm{step}(y - W_k) = [\mathrm{sgn}(y - W_k) + 1]/2$, $\mathrm{step}(-y - W_k) = [\mathrm{sgn}(-y - W_k) + 1]/2$, $\mathrm{sgn}(y)$ is a sign function. Furthermore, from Eqs. (5)–(7) with expression (8), when M is determined, the generated maximum wing can reach $N = 2M + 2$. The unified single parameter ε step function controller is shown in Fig. 3.

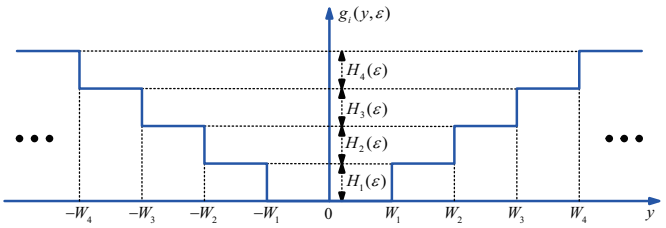


Fig. 3. (color online) A unified single parameter ε even-symmetric step function switching controller $g_i(y,\varepsilon)$.

2.3. Construction criterion for unified single parameter ε even-symmetric step function

Given W_k $(k = 1,2,\ldots,M)$, the construction criterion for unified single parameter ε even-symmetric step function is described by the following two aspects.

(i) As for $g_1(y,\varepsilon)$ in Eq. (5), the altitudes $H_k(\varepsilon)$ in expression (8) are determined by

$$\begin{cases} H_1(\varepsilon) = H_0 W_1 - \varepsilon, \\ H_2(\varepsilon) = H_0(W_2 - W_1) - \varepsilon, \\ H_3(\varepsilon) = H_0(W_3 - W_2) - \varepsilon, \\ \quad\vdots \\ H_M(\varepsilon) = H_0(W_M - W_{M-1}) - \varepsilon, \end{cases} \tag{9}$$

where $H_0 = a_{31}$, $W_1 = 0.5$, $W_2 = 1.0$, …, $W_m - W_{m-1} = 0.5$ $(m = 2,3,\ldots,M)$, and $\varepsilon = 0.32$. When $H_k(\varepsilon)$ are determined, to ensure that the absolute function $a_{31}|y|$ and step function $g_1(y,\varepsilon)$ as shown in Fig. 4 are not intersected, one can obtain the equations to determine the ε value range as

$$\begin{cases} a_{31}|y_1| - H_1 = a_{31}W_1 - (H_0 W_1 - \varepsilon) = \delta_1, & (0 < \delta_1 < H_1), \\ a_{31}|y_m| - \sum_{i=1}^{m} H_i = a_{31}W_m - \left\{(H_0 W_1 - \varepsilon) + \sum_{i=2}^{m}[H_0(W_i - W_{i-1})] - m\varepsilon\right\} = \delta_m, & (0 < \delta_m < H_m), \end{cases} \tag{10}$$

where $m = 2,3,4,\ldots,M$.

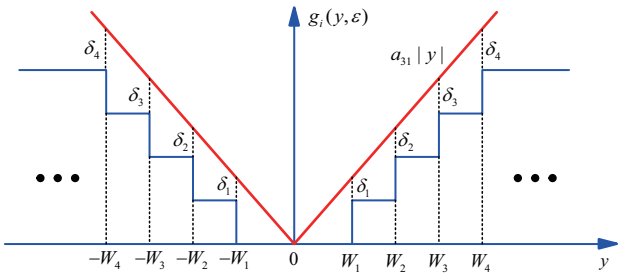


Fig. 4. (color online) Schematic diagram of disjunction between absolute value function $a_{31}|y|$ and step function $g_1(y,\varepsilon)$.

(ii) As for $g_2(y,\varepsilon)$ and $g_3(y,\varepsilon)$in Eqs. (6) and (7), the altitudes $H_k(\varepsilon)$ in Eq. (8) are determined by

$$\begin{cases} H_1(\varepsilon) = H_0 W_1^2 + \varepsilon, \\ H_2(\varepsilon) = H_0(W_2^2 - W_1^2) + \varepsilon, \\ H_3(\varepsilon) = H_0(W_3^2 - W_2^2) + \varepsilon, \\ \quad\vdots \\ H_M(\varepsilon) = H_0(W_M^2 - W_{M-1}^2) + \varepsilon. \end{cases} \tag{11}$$

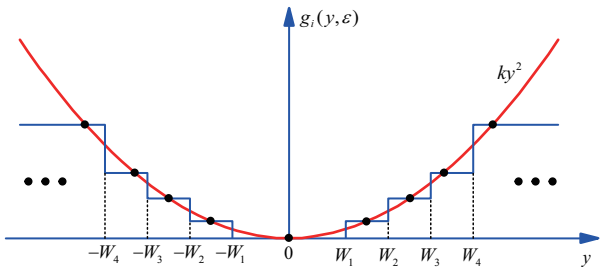


Fig. 5. (color online) Schematic diagram of intersection in each interval (W_{i-1}, W_i) between square function $ky^2 (k \in \{d_{31}, b_{41}\})$ and step function $g_i(y,\varepsilon)$ $(i = 2,3)$.

For $g_2(y,\varepsilon)$, let $H_0 = d_{31}$, $W_1 = 0.3$, $W_2 = 0.45$, …, $W_m - W_{m-1} = 0.15$ $(m = 2,3,\ldots,M)$, and $\varepsilon = 1.3$. For $g_3(y,\varepsilon)$, let $H_0 = b_{41}$, $W_1 = 1.0$, $W_2 = 1.5$, …, $W_m - W_{m-1} = 0.5$ $(m = 2,3,\ldots,M)$, and $\varepsilon = 1.3$. When $H_k(\varepsilon)$ are determined, to ensure that there is an intersection between square function $ky^2 (k \in \{d_{31}, b_{41}\})$ and step function $g_i(y,\varepsilon)(i = 1,2)$ in each interval (W_{i-1}, W_i) as shown in Fig. 5, one can obtain the equations to determine the ε value range as

$$\begin{cases} H_1 = H_0 W_1^2 + \varepsilon = k y_1^2, & (W_1 < y_1 < W_2), \\ \sum\limits_{i=1}^{m} H_i = (H_0 W_1^2 + \varepsilon) + \sum\limits_{i=2}^{m} [H_0 (W_i^2 - W_{i-1}^2)] \\ \qquad + m\varepsilon = k y_m^2, & (W_m < y_m < W_{m+1}), \end{cases} \tag{12}$$

where $m = 2,3,4,\ldots,M$.

2.4. Simulation results of multi-wing chaotic and hyperchaotic attractors

Let $M = 4$, according to Eqs. (5)–(12), one obtains the numerical simulation results of absolute value piecewise linear 3D 10-wing chaotic attractor, square 3D 10-wing chaotic attractor and square 4D 10-wing hyperchaotic attractor as shown in Fig. 6, respectively. The Lyapunov exponents of the absolute value piecewise linear 3D double 10-wing chaotic system are $\mathrm{LE}_1 = 0.27$, $\mathrm{LE}_2 = 0.00$, $\mathrm{LE}_3 = -0.92$, the Lyapunov exponents of the square 3D 10-wing chaotic system are $\mathrm{LE}_1 = 1.46$, $\mathrm{LE}_2 = 0.00$, and $\mathrm{LE}_3 = -20.45$, and the Lyapunov exponents of the square 4D 10-wing hyperchaotic system are $\mathrm{LE}_1 = 1.28$, $\mathrm{LE}_2 = 0.49$, $\mathrm{LE}_3 = 0.00$, and $\mathrm{LE}_4 = -20.46$, respectively.

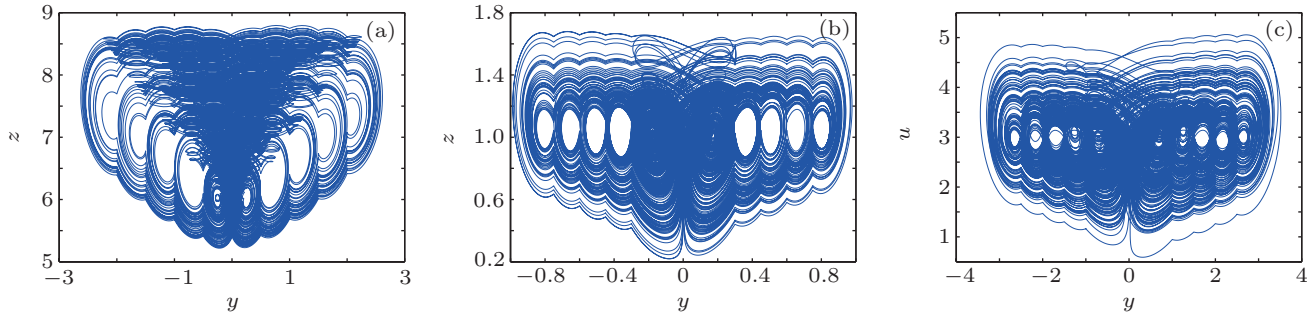


Fig. 6. (color online) 10-wing attractors of chaotic and hyperchaotic systems: (a) 10-wing attractor of absolute value piecewise linear 3D chaotic system; (b) 10-wing attractor of square 3D chaotic system; (c) 10-wing attractor of square 4D hyperchaotic system.

3. Dynamical properties of multi-wing system

In this section, the dynamical properties of multi-wing chaotic and hyperchaotic systems generated by the unified step function control are analyzed, including the equilibria of three types of multi-wing systems, non-equilibrium square 4D multi-wing hyperchaotic system, the mechanism analysis for piecewise linear 3D double wing and multi-wing chaotic system, mirror symmetry of multi-wing chaotic system, and the solution of absolute value piecewise linear 3D multi-wing chaotic system.

3.1. Equilibrium points

According to Eq. (5), one obtains the equilibria $P_{\pm q} = (x_{\pm q}^{(\mathrm{e})}, y_{\pm q}^{(\mathrm{e})}, z_{\pm q}^{(\mathrm{e})})$ of the absolute value piecewise linear 3D multi-wing chaotic system as

$$\begin{cases} x_0^{(\mathrm{e})} = y_0^{(\mathrm{e})} = z_0^{(\mathrm{e})} = 0, \quad x_{\pm q}^{(\mathrm{e})} = \frac{a_{12}}{a_{11}} y_{\pm q}^{(\mathrm{e})}, \\ y_{\pm q}^{(\mathrm{e})} = \pm \left(a_{21} a_{32} + \sum\limits_{i=1}^{q-1} H_i \right) / (a_{31} - a_{22} a_{32}), \\ z_{\pm q}^{(\mathrm{e})} = (a_{31}/a_{32}) |y_{\pm q}^{(\mathrm{e})}| - \left(\sum\limits_{i=1}^{q-1} H_i \right) / a_{32}, \end{cases} \tag{13}$$

where $q = 1,2,3,\ldots$, when $q = 1$, $\sum\limits_{i=1}^{q-1} H_i = 0$.

According to Eq. (6), one obtains the equilibria $P_{\pm q} = (x_{\pm q}^{(\mathrm{e})}, y_{\pm q}^{(\mathrm{e})}, z_{\pm q}^{(\mathrm{e})})$ of the square 3D multi-wing chaotic system as

$$\begin{cases} x_0^{(\mathrm{e})} = y_0^{(\mathrm{e})} = z_0^{(\mathrm{e})} = 0, \quad x_{\pm q}^{(\mathrm{e})} = \dfrac{d_{12}}{d_{11}} y_{\pm q}^{(\mathrm{e})}, \\ y_{\pm q}^{(\mathrm{e})} = \pm \sqrt{\dfrac{d_{11} d_{22} d_{32}}{d_{12} d_{21} d_{31}} + \left(\sum\limits_{i=1}^{q-1} H_i \right)} / d_{31}, \\ z_{\pm q}^{(\mathrm{e})} = \dfrac{d_{11} d_{22}}{d_{12} d_{21}}, \end{cases} \tag{14}$$

where $q = 1,2,3,\ldots$, when $q = 1$, $\sum\limits_{i=1}^{q-1} H_i = 0$.

According to Eq. (7), one obtains the equilibria $P_{\pm q} = (x_{\pm q}^{(\mathrm{e})}, y_{\pm q}^{(\mathrm{e})}, z_{\pm q}^{(\mathrm{e})})$ of the square 4D multi-wing hyperchaotic system as

$$\begin{cases} x_0^{(\mathrm{e})} = y_0^{(\mathrm{e})} = z_0^{(\mathrm{e})} = u_0^{(\mathrm{e})} = 0, \\ x_{\pm q}^{(\mathrm{e})} = \left(\dfrac{b_{12} b_{21} b_{32} - b_{13} b_{22} b_{31}}{b_{11} b_{21} b_{32}} \right) y_{\pm q}^{(\mathrm{e})}, \\ y_{\pm q}^{(\mathrm{e})} = \pm \sqrt{\dfrac{b_{42}}{b_{41}} \dfrac{b_{11} b_{22} b_{32}}{b_{12} b_{21} b_{32} - b_{13} b_{22} b_{31}} + \dfrac{1}{b_{41}} \sum\limits_{i=1}^{q-1} H_i}, \\ z_{\pm q}^{(\mathrm{e})} = -\dfrac{b_{22} b_{31}}{b_{21} b_{32}} y_{\pm q}^{(\mathrm{e})}, \\ u_{\pm q}^{(\mathrm{e})} = \dfrac{b_{11} b_{22} b_{32}}{b_{12} b_{21} b_{32} - b_{13} b_{22} b_{31}}, \end{cases} \tag{15}$$

where $q = 1, 2, 3, \ldots$, when $q = 1$, $\sum_{i=1}^{q-1} H_i = 0$.

3.2. Non-equilibrium square 4D multi-wing hyperchaotic system

According to Eq. (13), since $a_{ij} > 0$, $H_i > 0$, and they are all real numbers, one can deduce that the coordinates of equilibria $x_{\pm q}^{(e)}$, $y_{\pm q}^{(e)}$, and $z_{\pm q}^{(e)}$ are all real numbers, indicating that all of the equilibria really exist.

Similarly, according to Eq. (14), since $d_{ij} > 0$, $H_i > 0$, and they are all real numbers, one can deduce that the coordinates of equilibria $x_{\pm q}^{(e)}$, $y_{\pm q}^{(e)}$, and $z_{\pm q}^{(e)}$ are all real numbers, which means that all of the equilibria really exist.

In Eq. (15), if the following inequality holds:

$$\frac{b_{42}}{b_{41}} \frac{b_{11}b_{22}b_{32}}{b_{12}b_{21}b_{32} - b_{13}b_{22}b_{31}} + \frac{1}{b_{41}} \sum_{i=1}^{q-1} H_i > 0, \tag{16}$$

the coordinates of equilibria are all real numbers, which means that the equilibria really exist.

However, in Eq. (15), if the following inequality holds:

$$\frac{b_{42}}{b_{41}} \frac{b_{11}b_{22}b_{32}}{b_{12}b_{21}b_{32} - b_{13}b_{22}b_{31}} + \frac{1}{b_{41}} \sum_{i=1}^{q-1} H_i < 0, \tag{17}$$

the coordinates of equilibria are all imaginary numbers, which means that the equilibria do not exist.

From inequality (17), when the equilibria do not exist, the corresponding range of parameter b_{13} can be determined by

$$b_{13} > \frac{b_{11}b_{32}b_{42}}{b_{31} \sum_{i=1}^{q-1} H_i} + \frac{b_{12}b_{21}b_{32}}{b_{22}b_{31}}, \tag{18}$$

where $q = 5$, $n = 4$, $b_{11} = 36$, $b_{12} = 45$, $b_{21} = 5.6$, $b_{22} = 20$, $b_{31} = 0.5$, $b_{32} = 0.3$, $b_{41} = 17.9$, $b_{42} = 3$, $H_0 = 17.9$, $W_1 = 1.0$, $W_2 = 1.5$, $W_3 = 2.0$, $W_4 = 2.5$, and $\varepsilon = 1.3$. Also from Eq. (11), one obtains $H_1 = 19.2$, $H_2 = 23.675$, $H_3 = 32.625$, and $H_4 = 41.575$.

Substituting the above-mentioned parameters into inequality (18), one obtains

$$\frac{b_{11}b_{32}b_{42}}{b_{31} \sum_{i=1}^{q-1} H_i} + \frac{b_{12}b_{21}b_{32}}{b_{22}b_{31}} = 8.1135.$$

When $b_{13} > 8.1135$, equation (7) is a non-equilibrium multi-wing hyperchaotic system. Let $b_{13} = 9.0 > 8.1135$, the remaining parameters are the same as the above. The numerical simulation result of non-equilibrium 10-wing hyperchaotic attractor is shown in Fig. 7, and the corresponding Lyapunov exponents are $\mathrm{LE}_1 = 1.14$, $\mathrm{LE}_2 = 0.17$, $\mathrm{LE}_3 = 0.00$, and $\mathrm{LE}_4 = -19.98$. Furthermore, the Lyapunov exponents with parameter b_{13} variation are also obtained as shown in Fig. 8. Therefore, when $b_{13} < 8.1135$, equation (7) is an equilibrium multi-wing hyperchaotic system. However, when $b_{13} > 8.1135$, it is a non-equilibrium multi-wing hyperchaotic system.

As is well known, the equilibrium point is very important for a chaotic system. Based on the Shilnikov theorem, the key to forming heteroclinic orbit or heteroclinic loop is the existence of one or more saddle focus equilibria in the chaotic system. For example, in a generalized Lorenz system family, double-wing chaotic attractors can be formed from the saddle points or saddle focus points, and multi-wing chaotic attractors can be further formed from extending the number of saddle-focus equilibria. However, without equilibria, the homoclinic orbit or heteroclinic loop cannot be formed. The mechanism for such a kind of non-equilibrium hyperchaotic system needs to be further investigated in depth.

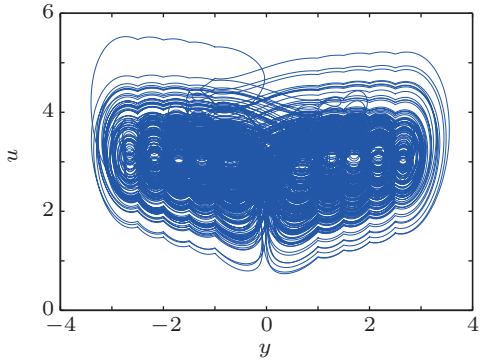


Fig. 7. (color online) Non-equilibrium 10-wing hyperchaotic attractor with $b_{13} = 9.0$.

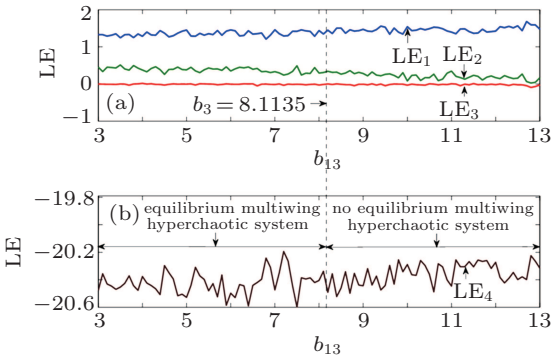


Fig. 8. (color online) (a) Positive and zero Lyapunov exponents; (b) negative Lyapunov exponent.

3.3. Chaotic mechanism analysis of double wing and multi-wing systems

In this section, according to the heteroclinic Shilnikov theorem, the chaotic mechanism analyses for absolute piecewise linear 3D double wing and multi-wing systems are given.

3.3.1. Chaotic mechanism analysis of double wing system

From Eqs. (2) and (13), one obtains the equilibria of absolute piecewise linear 3D chaotic system as follows:

$$\begin{cases} P_0 = (x_0^{(e)}, y_0^{(e)}, z_0^{(e)}) = (0, 0, 0), \\ P_{\pm 1} = (x_{\pm 1}^{(e)}, y_{\pm 1}^{(e)}, z_{\pm 1}^{(e)}) = (\pm 0.2518, \pm 0.2518, 5.9963). \end{cases} \tag{19}$$

The corresponding eigenvalues of the equilibria $P_{\pm 1} = (x_{\pm 1}^{(e)}, y_{\pm 1}^{(e)}, z_{\pm 1}^{(e)})$ are $\gamma = -1.18$, $\sigma \pm \mathrm{j}\omega = 0.266 \pm \mathrm{j}1.9523$,

which confirms that $P_{\pm1}=(x^{(e)}_{\pm1},y^{(e)}_{\pm1},z^{(e)}_{\pm1})$ are saddle-focus equilibria with index 2. Furthermore, one can further obtain the eigenvectors $(l_{\pm1},m_{\pm1},n_{\pm1})$ for one-dimensional (1D) stable manifold and $(A_{\pm1},B_{\pm1},C_{\pm1})$ for two-dimensional (2D) unstable manifold at the equilibria $P_{\pm1}=(x^{(e)}_{\pm1},y^{(e)}_{\pm1},z^{(e)}_{\pm1})$, respectively.

According to heteroclinic Shilnikov theorem, $P_{-1}=(x^{(e)}_{-1},y^{(e)}_{-1},z^{(e)}_{-1})$ and $P_{+1}=(x^{(e)}_{+1},y^{(e)}_{+1},z^{(e)}_{+1})$ are two different equilibria of 3D system, and the system is chaotic in the sense of Smale horseshoe if it satisfies the following two conditions.[12]

(i) Equilibria P_{-1} and P_{+1} are saddle-focus type and satisfy Shilnikov inequalities $|\gamma_i|>|\sigma_i|>0$ $(i=1,2)$, $\sigma_1\sigma_2>0$, and $\gamma_1\gamma_2>0$.

(ii) There is a heteroclinic loop connecting two equilibria P_{-1} and P_{+1}, which consists of two heteroclinic orbits HL_i $(i=1,2)$.

The 1D stable manifold $E^{\mathrm{S}}(P_{+1})$ and the 2D unstable manifold $E^{\mathrm{U}}(P_{+1})$ of $P_{+1}=(x^{(e)}_{+1},y^{(e)}_{+1},z^{(e)}_{+1})\in V_{+1}$ are given by

$$\begin{cases} E^{\mathrm{S}}(P_{+1}):\dfrac{x-x^{(e)}_{+1}}{l_{+1}}=\dfrac{y-y^{(e)}_{+1}}{m_{+1}}=\dfrac{z-z^{(e)}_{+1}}{n_{+1}},\\ E^{\mathrm{U}}(P_{+1}):A_{+1}(x-x^{(e)}_{+1})+B_{+1}(y-y^{(e)}_{+1})\\ \quad +C_{+1}(z-z^{(e)}_{+1})=0, \end{cases} \tag{20}$$

where l_{+1}, m_{+1}, and n_{+1} are three components of eigenvector of 1D stable manifold, A_{+1}, B_{+1}, and C_{+1} are three components of eigenvector of 2D unstable manifold.

Similarly, the 1D stable manifold $E^{\mathrm{S}}(P_{-1})$ and the 2D unstable manifold $E^{\mathrm{U}}(P_{-1})$ of $P_{-1}=(x^{(e)}_{-1},y^{(e)}_{-1},z^{(e)}_{-1})\in V_{-1}$ are given by

$$\begin{cases} E^{\mathrm{S}}(P_{-1}):\dfrac{x-x^{(e)}_{-1}}{l_{-1}}=\dfrac{y-y^{(e)}_{-1}}{m_{-1}}=\dfrac{z-z^{(e)}_{-1}}{n_{-1}},\\ E^{\mathrm{U}}(P_{-1}):A_{-1}(x-x^{(e)}_{-1})\\ \quad +B_{-1}(y-y^{(e)}_{-1})+C_{-1}(z-z^{(e)}_{-1})=0, \end{cases} \tag{21}$$

where l_{-1}, m_{-1}, and n_{-1} are three components of the eigenvector of 1D stable manifold, A_{-1}, B_{-1}, and C_{-1} are three components of the eigenvector of 2D unstable manifold.

According to Eqs. (20)–(21), one obtains the characteristic lines of 1D stable manifolds $E^{\mathrm{S}}(P_{+1})$ and $E^{\mathrm{S}}(P_{-1})$, and the characteristic planes of 2D unstable manifolds $E^{\mathrm{U}}(P_{+1})$ and $E^{\mathrm{U}}(P_{-1})$ as shown in Fig. 9, respectively, where $S_0(y)=\{(x,y,z)|y=0\}$ is switching plane. From Fig. 9, cross point Q_{+0} between $E^{\mathrm{S}}(P_{+1})$ and $S_0(y)=\{(x,y,z)|y=0\}$, Q_{-0} between $E^{\mathrm{S}}(P_{-1})$ and $S_0(y)$, cross lines L_{+0} and L_{-0} between $E^{\mathrm{U}}(P_{+1})$ and $S_0(y)$, and L_{-0} between $E^{\mathrm{U}}(P_{-1})$ and $S_0(y)$ can be further determined. In Fig. 9, switching plane $S_0(y)$ and switching region $V_{\pm1}(x,y,z)$ are obtained by

$$\begin{cases} S_0(y)=\{(x,y,z)|y=0\},\\ V_{+1}(x,y,z)=\{(x,y,z)|y>0\},\\ V_{-1}(x,y,z)=\{(x,y,z)|y<0\}. \end{cases} \tag{22}$$

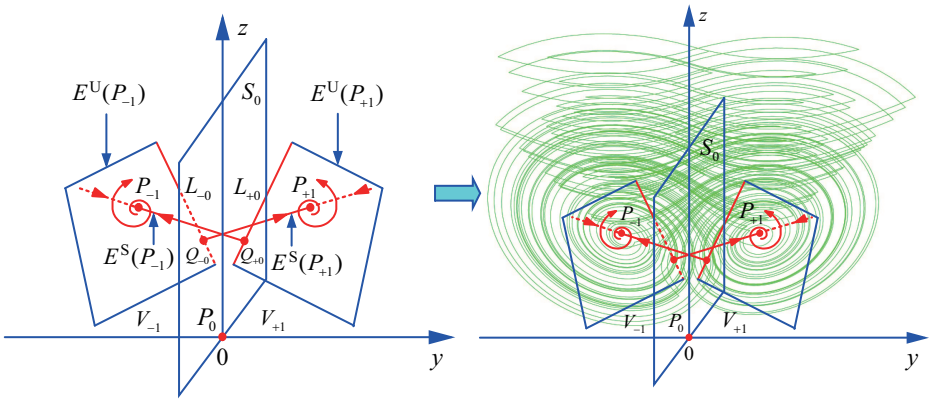


Fig. 9. (color online) Heteroclinic loop connecting two equilibria in absolute piecewise linear 3D double-wing chaotic system.

If Q_{+0} lies on L_{+0}, there is a heteroclinic orbit $\mathrm{HL}_1=E^{\mathrm{U}}(P_{+1})\cup Q_{+0}\cup E^{\mathrm{S}}(P_{-1})$ from P_{+1} to P_{-1}. Similarly, if Q_{-0} lies on L_{-0}, there is a heteroclinic orbit $\mathrm{HL}_2=E^{\mathrm{U}}(P_{-1})\cup Q_{-0}\cup E^{\mathrm{S}}(P_{+1})$ from P_{-1} to P_{+1}. By choosing a_{ij} in Eq. (2) and switching control parameters, if Q_{+0} lies in L_{+0} and Q_{-0} lies in L_{-0}, then there is a heteroclinic loop $HL=HL_1\cup HL_2=E^{\mathrm{U}}(P_{+1})\cup Q_{+0}\cup E^{\mathrm{S}}(P_{-1})\cup E^{\mathrm{U}}(P_{-1})\cup Q_{-0}\cup E^{\mathrm{S}}(P_{+1})$ connecting P_1 and P_2 together as shown in Fig. 9. Obviously, according to the heteroclinic Shilnikov theorem, equation (2) is chaotic in the sense of Smale horseshoe.

3.3.2. Chaotic mechanism analysis of multi-wing system

Equipped with the controller $g_1(y,\varepsilon)$, system (5) is a piecewise linear switching system, each switching plane $S_{\pm q}(y)$ and each switching region $V_{\pm q}(x,y,z)$ are given by

$$\begin{cases} S_0(y) = \{(x,y,z)|y=0\}, \\ S_{\pm q}(y) = \{(x,y,z)|y=\pm W_q\}, \\ V_{+1}(x,y,z) = \{(x,y,z)|y>0\}, \\ V_{-1}(x,y,z) = \{(x,y,z)|y<0\}, \\ V_{+q}(x,y,z) = \{(x,y,z)|S_{+(q-1)}(y)<y<S_{+q}(y)\}, \\ V_{-q}(x,y,z) = \{(x,y,z)|S_{-q}(y)<y<S_{-(q-1)}(y)\}, \end{cases} \tag{23}$$

where $q = 2,3,\ldots$.

According to Eqs. (5) and (13), one has the equilibrium regions of $V_{\pm q}(x,y,z)$ for absolute value piecewise linear 3D multi-wing chaotic system as

$$\begin{cases} P_0 = (x_0^{(e)}, y_0^{(e)}, z_0^{(e)}) = (0,0,0), \\ P_{\pm 1} = (x_{\pm 1}^{(e)}, y_{\pm 1}^{(e)}, z_{\pm 1}^{(e)}) \\ \quad = (\pm 0.2518, \pm 0.2518, 5.9963) \in V_{\pm 1}, \\ P_{\pm 2} = (x_{\pm 2}^{(e)}, y_{\pm 2}^{(e)}, z_{\pm 2}^{(e)}) \\ \quad = (\pm 0.6846, \pm 0.6846, 6.2992) \in V_{\pm 2}, \\ P_{\pm 3} = (x_{\pm 3}^{(e)}, y_{\pm 3}^{(e)}, z_{\pm 3}^{(e)}) \\ \quad = (\pm 1.1173, \pm 1.1173, 6.6021) \in V_{\pm 3}, \\ P_{\pm 4} = (x_{\pm 4}^{(e)}, y_{\pm 4}^{(e)}, z_{\pm 4}^{(e)}) \\ \quad = (\pm 1.5500, \pm 1.5500, 6.9050) \in V_{\pm 4}. \\ \quad \ldots\ldots \end{cases} \tag{24}$$

In system (5), except for $O(0,0,0)$, there are the three same eigenvalues $\gamma = -1.18$, $\sigma \pm \mathrm{j}\omega = 0.266 \pm \mathrm{j}\,1.9523$ of equilibria in each linear region $V_{\pm q}$. Therefore, these equilibria are saddle-focus equilibria with index 2. One has the 1D stable manifold $E^{\mathrm{S}}(P_{\pm q})$ and 2D unstable manifold $E^{\mathrm{U}}(P_{\pm q})$ of $P_{\pm q} = (x_{\pm q}^{(e)}, y_{\pm q}^{(e)}, z_{\pm q}^{(e)}) \in V_{\pm q}$ $(q = 1,2,\ldots)$ as follows:

$$\begin{cases} E^{\mathrm{S}}(P_{\pm q}) : \dfrac{x - x_{\pm q}^{(e)}}{l_{\pm q}} = \dfrac{y - y_{\pm q}^{(e)}}{m_{\pm q}} = \dfrac{z - z_{\pm q}^{(e)}}{n_{\pm q}}, \\ E^{\mathrm{U}}(P_{\pm q}) : A_{\pm q}(x - x_{\pm q}^{(e)}) + B_{\pm q}(y - y_{\pm q}^{(e)}) \\ \quad + C_{\pm q}(z - z_{\pm q}^{(e)}) = 0, \end{cases} \tag{25}$$

where $l_{\pm q}$, $m_{\pm q}$, and $n_{\pm q}$ are three components of the eigenvector of 1D stable manifold; $A_{\pm q}$, $B_{\pm q}$, and $C_{\pm q}$ are three components of the eigenvector of 2D unstable manifold.

Based on Eq. (25), one further obtains the characteristic lines of 1D stable manifolds $E^{\mathrm{S}}(P_{\pm q})$ and the characteristic planes of 2D unstable manifolds $E^{\mathrm{U}}(P_{\pm q})$ as shown in Fig. 10. The cross points $Q_{\pm m}$ $(m = 0,1,2,3,\ldots)$ between $E^{\mathrm{S}}(P_{\pm q})$, $S_0(y)$, and $S_{\pm q}(y)$, and cross lines $L_{\pm m}$ $(m = 0,1,2,3,\ldots)$ between $E^{\mathrm{U}}(P_{\pm q})$, $S_0(y)$, and $S_{\pm q}(y)$ can be obtained.

By choosing a_{ij} in Eq. (5) and switching control parameters, all $Q_{\pm m}$ lie on $L_{\pm m}$, then there is a heteroclinic loop connecting two adjacent equilibria together as shown in Fig. 10. Obviously, according to the heteroclinic Shilnikov theorem, equation (5) is chaotic in the sense of Smale horseshoe.[25]

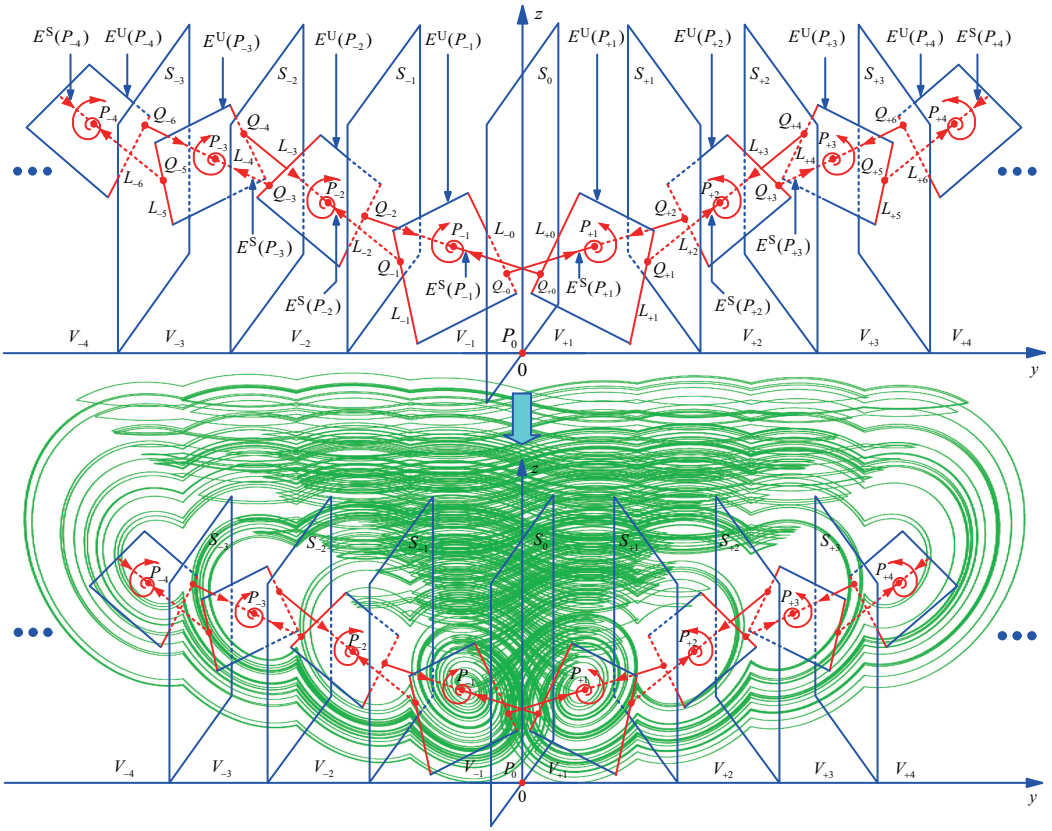


Fig. 10. (color online) Multiple heteroclinic loops connecting multiple adjacent equilibria in absolute piecewise linear 3D multi-wing chaotic system.

3.4. Mirror symmetry

Theorem 1 Assume that the general form of 3D multi-wing chaotic system family is

$$\begin{cases} \dot{x} = f_1(x,y,z), \\ \dot{y} = f_2(x,y,z), \\ \dot{z} = \xi_{n1}h(y) - \xi_{n2}z - g(y), \end{cases} \tag{26}$$

where $h(y) \in \{|y|, y^2\}$ is an even-symmetric function, ξ_{n1} and ξ_{n2} are constants, and $g(y)$ is a step function switching controller.

If the corresponding conversion of Eq. (26) with respect to the z axis is given by

$$\begin{cases} \dot{x} = f_1(x,y,|z| \pm z_0), \\ \dot{y} = f_2(x,y,|z| \pm z_0), \\ \dot{z} = \mathrm{sgn}(z)[\xi_{n1}h(y) - \xi_{n2}(|z| \pm z_0) - g(y)], \end{cases} \tag{27}$$

then the solution of Eq. (27) is of mirror symmetry with respect to the z axis. In Eq. (27), z_0 is a coordinate translation constant, which makes the solution of Eq. (26) always satisfy $z \geq 0$ (or $z \leq 0$).

Proof According to Eq. (27), one can obtain its solution of the integral form as follows:

$$\begin{cases} x = \int_{-\infty}^{t} f_1(x(\tau),y(\tau),|z(\tau)| \pm z_0)\,\mathrm{d}\tau, \\ y = \int_{-\infty}^{t} f_2(x(\tau),y(\tau),|z(\tau)| \pm z_0)\,\mathrm{d}\tau, \\ z = \int_{-\infty}^{t} sgn(z(\tau))[\xi_{n1}h(y(\tau)) - \xi_{n2}(|z(\tau)| \pm z_0) - g(y)]\,\mathrm{d}\tau. \end{cases} \tag{28}$$

Obviously, if $z(\tau) > 0$, the solution of the integral form is given by

$$\begin{cases} x = \int_{-\infty}^{t} f_1(x(\tau),y(\tau),|z(\tau)| \pm z_0)\,\mathrm{d}\tau, \\ y = \int_{-\infty}^{t} f_2(x(\tau),y(\tau),|z(\tau)| \pm z_0)\,\mathrm{d}\tau, \\ z = \int_{-\infty}^{t} [\xi_{n1}h(y(\tau)) - \xi_{n2}(|z(\tau)| \pm z_0) - g(y)]\,\mathrm{d}\tau. \end{cases} \tag{29}$$

If $z(\tau) < 0$, the solution of the integral form is given by

$$\begin{cases} x = \int_{-\infty}^{t} f_1(x(\tau),y(\tau),|z(\tau)| \pm z_0)\,\mathrm{d}\tau, \\ y = \int_{-\infty}^{t} f_2(x(\tau),y(\tau),|z(\tau)| \pm z_0)\,\mathrm{d}\tau, \\ z = -\int_{-\infty}^{t} [\xi_{n1}h(y(\tau)) - \xi_{n2}(|z(\tau)| \pm z_0) - g(y)]\,\mathrm{d}\tau, \end{cases} \tag{30}$$

where

$$\begin{cases} f_1(x(\tau),y(\tau),z(\tau) \pm z_0)(z(\tau) > 0) \\ \equiv f_1(x(\tau),y(\tau),-z(\tau) \pm z_0)\ (z(\tau) < 0), \\ f_2(x(\tau),y(\tau),z(\tau) \pm z_0)(z(\tau) > 0) \\ \equiv f_2(x(\tau),y(\tau),-z(\tau) \pm z_0)\ (z(\tau) < 0), \\ \xi_{n1}h(y(\tau)) - \xi_{n2}(z(\tau) \pm z_0) - g(y)\ (z(\tau) > 0) \\ \equiv \xi_{n1}h(y(\tau)) + \xi_{n2}(z(\tau) \pm z_0) - g(y)(z(\tau) < 0). \end{cases}$$

According to Eqs. (29) and (30), one can see that the solution of Eq. (27) is of mirror symmetry with respect to the z axis. Therefore, the proof of the theorem 1 is completed.

For example, by using the mirror symmetry conversion, system (5) is modified into

$$\begin{cases} \dot{x} = -a_{11}x + a_{12}y, \\ \dot{y} = \mathrm{sgn}(x)[a_{21} - (|z| - z_0)] + a_{22}y, \\ \dot{z} = \mathrm{sgn}(z)[a_{31}|y| - a_{32}(z - z_0) - g_1(y)], \end{cases} \tag{31}$$

where $z_0 = 5.25$. From Eq. (31), the numerical simulation result of multi-wing chaotic attractor is shown in Fig. 11.

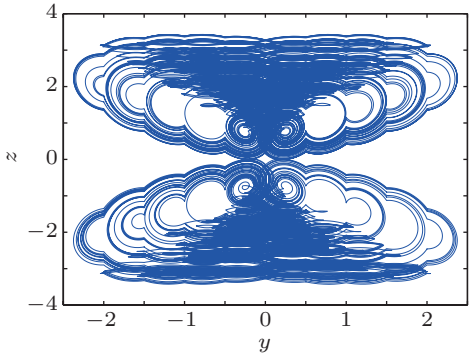


Fig. 11. (color online) Absolute value piecewise linear 3D 20-wing chaotic system after mirror symmetry conversion.

3.5. Solution of absolute value piecewise linear 3D chaotic system

3.5.1. Solution of absolute value piecewise linear 3D double wing chaotic system

In absolute value piecewise linear 3D double-wing chaotic equation (2), there are four linear regions, and the corresponding solutions of state equation can be obtained, respectively, as follows.

(i) When $x_1 > 0$, $y_1 > 0$, one has

$$\begin{pmatrix} x_1(t) \\ y_1(t) \\ z_1(t) \end{pmatrix} = \boldsymbol{P}_1 \begin{pmatrix} \mathrm{e}^{\gamma t} & 0 & 0 \\ 0 & \mathrm{e}^{\sigma t}\cos\omega t & \mathrm{e}^{\sigma t}\sin\omega t \\ 0 & -\mathrm{e}^{\sigma t}\sin\omega t & \mathrm{e}^{\sigma t}\cos\omega t \end{pmatrix} \times \boldsymbol{P}_1^{-1} \begin{pmatrix} x_1(0) \\ y_1(0) \\ z_1(0) \end{pmatrix} = \boldsymbol{M}_1 \begin{pmatrix} x_1(0) \\ y_1(0) \\ z_1(0) \end{pmatrix}, \tag{32}$$

where $\gamma = -1.18$, $\sigma = 0.266$, $\omega = 1.9523$,

$$\boldsymbol{P}_1 = \begin{pmatrix} 1 & 0.1939 & 0.0863 \\ 0 & 0.0948 & 0.4266 \\ 0 & 0.8740 & 0 \end{pmatrix},$$

$$\boldsymbol{P}_1^{-1} = \begin{pmatrix} 1 & -0.2023 & -0.1999 \\ 0 & 0 & 1.1442 \\ 0 & 2.3441 & -0.2543 \end{pmatrix},$$

and

$$\boldsymbol{M}_1 = \begin{pmatrix} \mathrm{e}^{\gamma t} & -0.2023\,\mathrm{e}^{\gamma t} + 0.4545\,\mathrm{e}^{\sigma t}\sin\omega t + 0.2023\,\mathrm{e}^{\sigma t}\cos\omega t & -0.1999\,\mathrm{e}^{\gamma t} - 0.148\,\mathrm{e}^{\sigma t}\sin\omega t + 0.2\,\mathrm{e}^{\sigma t}\cos\omega t \\ 0 & 0.2222\,\mathrm{e}^{\sigma t}\sin\omega t + \mathrm{e}^{\sigma t}\cos\omega t & -0.5122\,\mathrm{e}^{\sigma t}\sin\omega t \\ 0 & 2.0487\,\mathrm{e}^{\sigma t}\sin\omega t & \mathrm{e}^{\sigma t}\cos\omega t - 0.2223\,\mathrm{e}^{\sigma t}\sin\omega t \end{pmatrix}.$$

(ii) When $x_2 < 0$, $y_2 < 0$, one has

$$\begin{pmatrix} x_2(t) \\ y_2(t) \\ z_2(t) \end{pmatrix} = \boldsymbol{P}_2 \begin{pmatrix} \mathrm{e}^{\gamma t} & 0 & 0 \\ 0 & \mathrm{e}^{\sigma t}\cos\omega t & \mathrm{e}^{\sigma t}\sin\omega t \\ 0 & -\mathrm{e}^{\sigma t}\sin\omega t & \mathrm{e}^{\sigma t}\cos\omega t \end{pmatrix} \boldsymbol{P}_2^{-1} \begin{pmatrix} x_2(0) \\ y_2(0) \\ z_2(0) \end{pmatrix} = \boldsymbol{M}_2 \begin{pmatrix} x_2(0) \\ y_2(0) \\ z_2(0) \end{pmatrix}, \tag{33}$$

where $\gamma = -1.18$, $\sigma = 0.266$, $\omega = 1.9523$,

$$\boldsymbol{P}_2 = \begin{pmatrix} 1 & 0.1939 & 0.0863 \\ 0 & 0.0948 & 0.4266 \\ 0 & -0.8740 & 0 \end{pmatrix}, \quad \boldsymbol{P}_2^{-1} = \begin{pmatrix} 1 & -0.2023 & 0.1999 \\ 0 & 0 & -1.1442 \\ 0 & 2.3441 & 0.2543 \end{pmatrix},$$

and

$$\boldsymbol{M}_2 = \begin{pmatrix} \mathrm{e}^{\gamma t} & -0.2023\,\mathrm{e}^{\gamma t} + 0.4545\,\mathrm{e}^{\sigma t}\sin\omega t + 0.2023\,\mathrm{e}^{\sigma t}\cos\omega t & 0.1999\,\mathrm{e}^{\gamma t} + 0.0494\,\mathrm{e}^{\sigma t}\sin\omega t - 0.2438\,\mathrm{e}^{\sigma t}\cos\omega t \\ 0 & 0.2222\,\mathrm{e}^{\sigma t}\sin\omega t + \mathrm{e}^{\sigma t}\cos\omega t & -0.217\,\mathrm{e}^{\sigma t}\cos\omega t + 0.464\,\mathrm{e}^{\sigma t}\sin\omega t \\ 0 & -2.0487\,\mathrm{e}^{\sigma t}\sin\omega t & \mathrm{e}^{\sigma t}\cos\omega t + 0.2223\,\mathrm{e}^{\sigma t}\sin\omega t \end{pmatrix}.$$

(iii) When $x_3 > 0$, $y_3 < 0$, one has

$$\begin{pmatrix} x_3(t) \\ y_3(t) \\ z_3(t) \end{pmatrix} = \begin{pmatrix} \mathrm{e}^{\lambda_1 t}\bar{v}_{11} & \mathrm{e}^{\lambda_2 t}\bar{v}_{21} & \mathrm{e}^{\lambda_3 t}\bar{v}_{31} \\ \mathrm{e}^{\lambda_1 t}\bar{v}_{12} & \mathrm{e}^{\lambda_2 t}\bar{v}_{22} & \mathrm{e}^{\lambda_3 t}\bar{v}_{32} \\ \mathrm{e}^{\lambda_1 t}\bar{v}_{13} & \mathrm{e}^{\lambda_2 t}\bar{v}_{23} & \mathrm{e}^{\lambda_3 t}\bar{v}_{33} \end{pmatrix} \begin{pmatrix} \bar{c}_1 \\ \bar{c}_2 \\ \bar{c}_3 \end{pmatrix}, \tag{34}$$

where $\lambda_1 = -1.18$, $\lambda_2 = 2.3125$, $\lambda_3 = -1.7805$,

$$\begin{pmatrix} \bar{v}_{11} \\ \bar{v}_{12} \\ \bar{v}_{13} \end{pmatrix} = \begin{pmatrix} 1 \\ 0 \\ 0 \end{pmatrix}, \quad \begin{pmatrix} \bar{v}_{21} \\ \bar{v}_{22} \\ \bar{v}_{23} \end{pmatrix} = \begin{pmatrix} 0.1753 \\ 0.5189 \\ -0.8367 \end{pmatrix},$$

$$\begin{pmatrix} \bar{v}_{31} \\ \bar{v}_{32} \\ \bar{v}_{33} \end{pmatrix} \begin{pmatrix} -0.5921 \\ 0.3013 \\ 0.7474 \end{pmatrix},$$

$$\bar{c}_1 = x_3(0) + 0.5695y_3(0) + 0.5628z_3(0),$$

$$\bar{c}_2 = 1.1680y_3(0) - 0.4709z_3(0),$$

$$\bar{c}_3 = 1.3077y_3(0) + 0.8112z_3(0).$$

(iv) When $x_4 < 0$, $y_4 > 0$, one has

$$\begin{pmatrix} x_4(t) \\ y_4(t) \\ z_4(t) \end{pmatrix} = \begin{pmatrix} \mathrm{e}^{\lambda_1 t}\hat{v}_{11} & \mathrm{e}^{\lambda_2 t}\hat{v}_{21} & \mathrm{e}^{\lambda_3 t}\hat{v}_{31} \\ \mathrm{e}^{\lambda_1 t}\hat{v}_{12} & \mathrm{e}^{\lambda_2 t}\hat{v}_{22} & \mathrm{e}^{\lambda_3 t}\hat{v}_{32} \\ \mathrm{e}^{\lambda_1 t}\hat{v}_{13} & \mathrm{e}^{\lambda_2 t}\hat{v}_{23} & \mathrm{e}^{\lambda_3 t}\hat{v}_{33} \end{pmatrix} \begin{pmatrix} \hat{c}_1 \\ \hat{c}_2 \\ \hat{c}_3 \end{pmatrix}, \tag{35}$$

where $\lambda_1 = -1.18$, $\lambda_2 = 2.3125$, $\lambda_3 = -1.7805$,

$$\begin{pmatrix} \hat{v}_{11} \\ \hat{v}_{12} \\ \hat{v}_{13} \end{pmatrix} = \begin{pmatrix} 1 \\ 0 \\ 0 \end{pmatrix}, \quad \begin{pmatrix} \hat{v}_{21} \\ \hat{v}_{22} \\ \hat{v}_{23} \end{pmatrix} = \begin{pmatrix} 0.1753 \\ 0.5189 \\ 0.8367 \end{pmatrix},$$

$$\begin{pmatrix} \hat{v}_{31} \\ \hat{v}_{32} \\ \hat{v}_{33} \end{pmatrix} \begin{pmatrix} 0.5921 \\ -0.3013 \\ 0.7474 \end{pmatrix},$$

$$\hat{c}_1 = x_4(0) - 0.9791y_4(0) - 1.1868z_4(0),$$

$$\hat{c}_2 = 1.1680y_4(0) + 0.4709z_4(0),$$

$$\hat{c}_3 = 1.3076y_4(0) + 1.8651z_4(0).$$

3.5.2. Solution of absolute value piecewise linear 3D multi-wing chaotic system

It is noticed that the absolute value piecewise linear 3D multi-wing chaotic equation (5) is obtained through linear transformation of Eq. (2) by switching control. From Eqs. (32)–(35), the corresponding solution of state equation (5) is given by

$$\begin{pmatrix} x(t) \\ y(t) \\ z(t) \end{pmatrix} - \begin{pmatrix} x_{\pm q}^{(\mathrm{e})} \\ y_{\pm q}^{(\mathrm{e})} \\ z_{\pm q}^{(\mathrm{e})} \end{pmatrix} = \begin{cases} (x_1(t)y_1(t)z_1(t))^{\mathrm{T}}, & \text{if } (x_1 > 0,\ y_1 > 0), \\ (x_2(t)y_2(t)z_2(t))^{\mathrm{T}}, & \text{if } (x_2 < 0,\ y_2 < 0), \\ (x_3(t)y_3(t)z_3(t))^{\mathrm{T}}, & \text{if } (x_3 > 0,\ y_3 < 0), \\ (x_4(t)y_4(t)z_4(t))^{\mathrm{T}}, & \text{if } (x_4 < 0,\ y_4 > 0), \end{cases} \tag{36}$$

where $P_{\pm q}(x_{\pm q}^{(\mathrm{e})}, y_{\pm q}^{(\mathrm{e})}, z_{\pm q}^{(\mathrm{e})}) \in V_{\pm q}$ are equilibria, $q = 1, 2, 3, \ldots$, and symbol T is the transpose of matrix.

4. Circuit design and implementation

Based on Eqs. (5) and (6), the circuit diagrams are designed as shown in Figs. 12–14. When switch K_1 is at position 1 in Fig. 14, $q(y) = q_{\mathrm{C}}(y)$; when it is at position 2, $q(y) = q_{\mathrm{L}}(y)$. The values of resistance, comparative voltage, switch state, and number of wings, and also the types of chaotic system are given in Tables 1–3, respectively. Based on the circuits given in Figs. 12–14 and Tables 1–3, the experimental results are shown in Fig. 15.

Table 1. Resistance values and the types of chaotic system in Fig. 14.

R/kΩ	R_1kΩ	R_2/kΩ	R_3/kΩ	R_4/kΩ	Type of chaotic system
2.5	12.5	11	11	11	Eq. (5)
0.1	20	16.67	12	11	Eq. (6)

Table 2. Comparative voltages and the types of chaotic system in Fig. 14.

E_1	E_2	E_3	E_4	Type of chaotic system
0.5	1.0	1.5	2.0	Eq. (5)
0.3	0.45	0.6	0.75	Eq. (6)

Table 3. On-off for switch linkages K_2–K_4 and numbers of wings in Fig. 14.

K_2	K_3	K_4	Number of wing
off	off	off	4
on	off	off	6
on	on	off	8
on	on	on	10

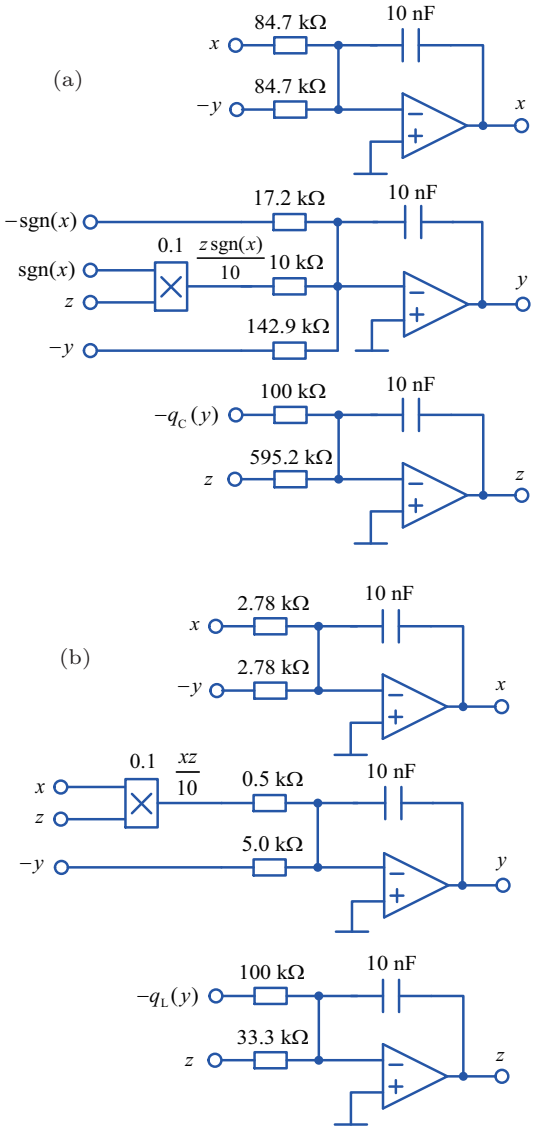


Fig. 12. (color online) Circuit diagrams of multi-wing chaotic systems: (a) the circuit diagram of absolute value piecewise linear 3D multi-wing chaotic system and (b) the circuit diagram of square 3D multi-wing chaotic system.

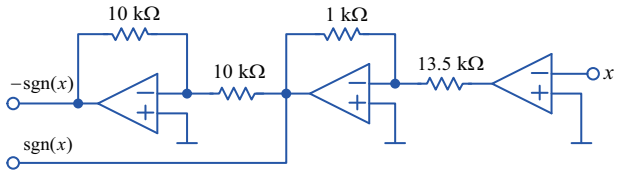


Fig. 13. (color online) Circuit design for sgn(x) of Fig. 12.

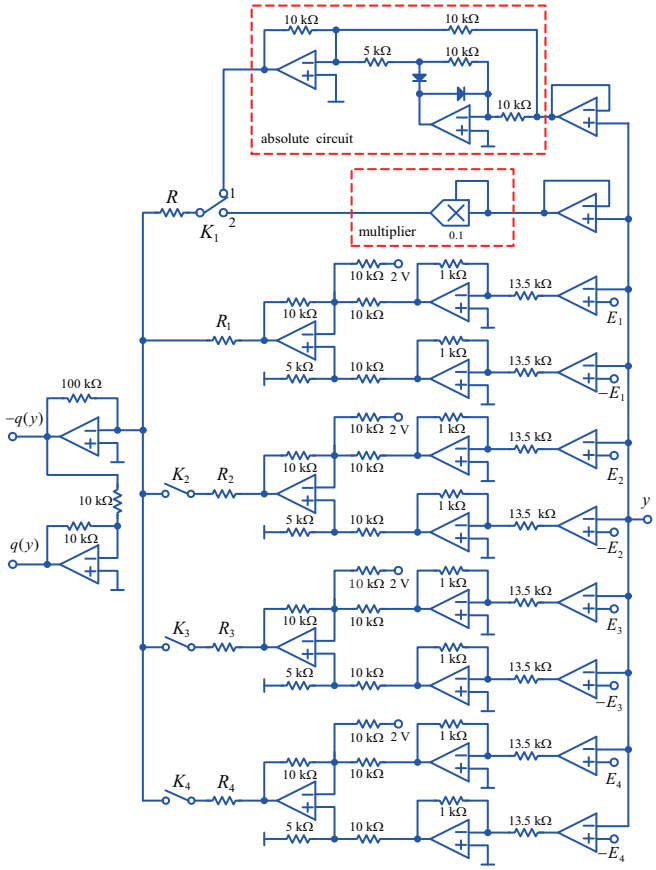


Fig. 14. (color online) Circuit design for nonlinear functions $q_C(y)$ and $q_L(y)$ of Fig. 12.

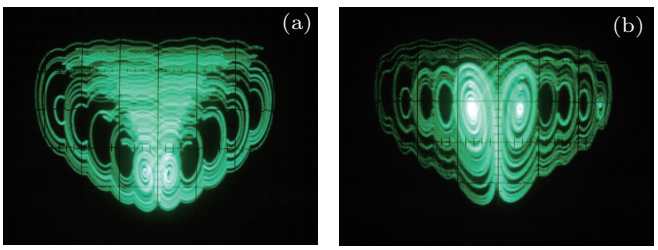


Fig. 15. (color online) Circuit experimental results: (a) experimental result of absolute value piecewise linear 3D 10-wing chaotic attractor and (b) experimental result of square 3D 10-wing chaotic attractor.

5. Conclusions

In this paper, we introduce a novel method of constructing multi-wing butterfly chaotic and hyperchaotic systems via a unified single parameter ε even-symmetric step function control, to overcome the essential difficulties in iteratively adjusting multiple parameters for a conventional multi-parameter control method. By using the proposed strategy, we further

find a non-equilibrium 4D multi-wing hyperchaotic system, which is valuable for future investigation due to the significance in basic research and importance in practical application. In addition, some properties for the multi-wing attractor and its chaos mechanism are also discussed and analyzed. The circuits for absolute piecewise linear 3D multi-wing system and for square 3D multi-wing system are designed and implemented for demonstration, respectively.

References

[1] Ott E, Grebogi C and Yorke J A 1990 *Phys. Rev. Lett.* **64** 1196
[2] Li X J and Zhou D H 2015 *Acta Phys. Sin.* **64** 140501 (in Chinese)
[3] Michael S, Marius F D and Aziz A M A 2015 *Chin. Phys. B* **24** 060507
[4] Chen G and Lai D 1998 *Int. J. Bifurc. Chaos* **8** 1585
[5] Wang F Q and Liu C X 2007 *Chin. Phys. B* **16** 0942
[6] Tang K S, Zhong G Q, Chen G and Man K F 2001 *IEEE Trans. Circuits Syst. I* **48** 1369
[7] Huang Y, Zhang P and Zhao W F 2015 *IEEE Trans. Circuits Syst. II* **62** 496
[8] Chen L, Shi Y D and Wang D S 2010 *Chin. Phys. B* **19** 0100503
[9] Bouallegue K, Chaari A and Toumi A 2010 *Chaos Solit. Fract.* **44** 79
[10] Yu S M, Tang W K S, Lü J H and Chen G 2008 *IEEE Trans. Circuits Syst. II* **55** 1168
[11] Zhou X, Wang C H and Guo X R 2012 *Acta Phys. Sin.* **61** 200506 (in Chinese)
[12] Luo X H, Tu Z W, Liu X R, Cai C, Liang Y L and Gong P 2010 *Chin. Phys. B* **19** 070510
[13] Lü J H and Chen G 2006 *Int. J. Bifurc. Chaos* **16** 775
[14] Silva C P 1993 *IEEE Trans Circuits Syst. I* **40** 675
[15] Lorenz E N 1963 *J. Atmos. Sci.* **20** 130
[16] Chen G R and Ueta T 1999 *Int. J. Bifurc. Chaos* **9** 1465
[17] Lü J H and Chen G R 2002 *Int. J. Bifurc. Chaos* **12** 659
[18] Lü J H, Chen G R and Cheng D 2004 *Int. J. Bifurc. Chaos* **14** 1507
[19] Tahir F R, Jafari S, Pham V T, Volos C and Wang X 2015 *Int. J. Bifurc. Chaos* **25** 1550056
[20] Sprott J C 1994 *Phys. Rev. E* **50** 647
[21] Wei Z 2011 *Phys. Lett. A* **376** 102
[22] Li C and Sprott J C 2014 *Int. J. Bifurc. Chaos* **24** 1450034
[23] Leonov G A, Kuznetsov N V and Vagaitsev V I 2012 *Physica D* **241** 1482
[24] Chaudhuri U and Prasad A 2014 *Phys. Lett. A* **378** 713
[25] Yu S M, Lü J H, Chen G R and Yu X H 2011 *IEEE Trans Circuits Syst. II* **58** 314